Protein NMR

International Edition: DOI: 10.1002/anie.201610441
German Edition: DOI: 10.1002/ange.201610441

Proton-Detected Solid-State NMR Spectroscopy of a Zinc Diffusion Facilitator Protein in Native Nanodiscs

Beate Bersch, Jonas M. Dörr, Audrey Hessel, J. Antoinette Killian, and Paul Schanda**

Abstract: *The structure, dynamics, and function of membrane proteins are intimately linked to the properties of the membrane environment in which the proteins are embedded. For structural and biophysical characterization, membrane proteins generally need to be extracted from the membrane and reconstituted in a suitable membrane-mimicking environment. Ensuring functional and structural integrity in these environments is often a major concern. The styrene/maleic acid co-polymer has recently been shown to be able to extract lipid/membrane protein patches directly from native membranes to form nanosize discoidal proteolipid particles, also referred to as native nanodiscs. In this work, we show that high-resolution solid-state NMR spectra can be obtained from an integral membrane protein in native nanodiscs, as exemplified by the 2 × 34 kDa bacterial cation diffusion facilitator CzcD.*

Structural and biophysical characterization of membrane proteins by most biophysical techniques generally requires extraction and purification from the native membrane. Major concerns when working with detergent-solubilized membrane proteins are related to the fact that functionally and structurally important lipids are often stripped away, and the properties of the detergent micelles differ significantly from the planar lipid bilayer environment. An increasing number of cases of distortions of membrane protein structures in detergents have been reported.[1,2] These known problems with detergents have triggered the development of alternative non-micellar systems, such as amphiphilic polymers (amphipols), bicelles, or nanolipoprotein particles, which consist of a lipid patch surrounded by a membrane-scaffold protein.[3–5] A particularly interesting recent approach is the use of the styrene/maleic acid co-polymer (SMA), which is able to self-insert into the lipid bilayer and extract membrane proteins directly from the membrane to form nanosized disc-shaped particles.[5–7] SMA has been successfully used to solubilize membrane proteins from reconstituted proteoliposomes,[8,9] and also from native cellular membranes, forming so-called native nanodiscs.[7,10–14] The stability and activity of proteins in SMA-bounded nanodiscs have been shown to be significantly higher than in detergent micelles in several instances, and some cases have been reported where the stability is even higher than in the native membrane.[15] These nanodiscs have been used in functional tests, ligand-binding studies, electron microscopy, EPR, and other spectroscopic characterizations methods (reviewed in Ref. [16]). Herein, we show that membrane proteins in native nanodiscs are amenable to atomic-resolution studies using magic-angle-spinning solid-state NMR (MAS ssNMR) spectroscopy. We demonstrate this with the integral membrane protein CzcD from *Cupriavidus metallidurans* CH34, a zinc diffusion facilitator with a molecular weight of 34 kDa. In *C. metallidurans* CH34, CzcD is part of a cobalt-zinc-cadmium resistance system (Czc).[17] Based on similarity to proteins of known structure, CzcD is assumed to form homodimers. Currently, structural information on full-length proteins of this family is available from two bacterial cation diffusion facilitator (CDF) proteins, one in an outward-facing state[18] (*Escherichia coli* Yiip, see homology model in Figure 1 a), the other in an inward-facing state[19] (*Shewanella oneidensis* YiiP). These structures may represent the two states of an alternate access mechanism. However, since this structural information has been obtained from protein reconstituted in detergent micelles[18] or tubular crystals,[19] characterization of the conformational change in response to Zn^{2+} ions in a more physiological membrane environment would be of great importance for the decryption of its transport mechanism. Direct solubilization in the form of native nanodiscs, combined with high-resolution solid-state NMR spectroscopy, would therefore be a promising approach for revealing the details of the way CDF proteins carry out cation transport across the membrane.

When expressed in *E. coli*, we found that CzcD was directly inserted into the cytoplasmic membrane. After cell lysis, the membrane fraction was isolated and incubated with SMA polymers (see Figures S1–S3 and detailed experimental methods in the Supporting Information). SMA-solubilized CzcD was purified using Strep-Tactin affinity chromatography, thereby demonstrating that this type of affinity purification can be successfully used for proteins solubilized with SMA. The Strep-tag was preferred over a His-tag because it does not interfere with metal binding to the protein. Figure 1 b shows a size-exclusion chromatography (SEC) profile of a nanodisc-embedded CzcD sample. The chromatogram shows two major peaks eluting at 48 and 67 mL, with a smaller shoulder at 58 mL. Negative-staining electron microscopy images of these three fractions are shown in Figure 1 c. The first protein-containing fraction contains relatively large,

[*] Dr. B. Bersch, A. Hessel, Dr. P. Schanda
CEA, CNRS, Univ. Grenoble Alpes
Institut de Biologie Structurale
71, avenue des martyrs, 38044 Grenoble (France)
E-mail: beate.bersch@ibs.fr
paul.schanda@ibs.fr
J. M. Dörr, J. A. Killian
Membrane Biochemistry and Biophysics
Bijvoet Center for Biomolecular Research, Utrecht University
Padualaan 8, 3584 CH Utrecht (The Netherlands)
Supporting information and the ORCID identification number(s) for the author(s) of this article can be found under http://dx.doi.org/10.1002/anie.201610441.

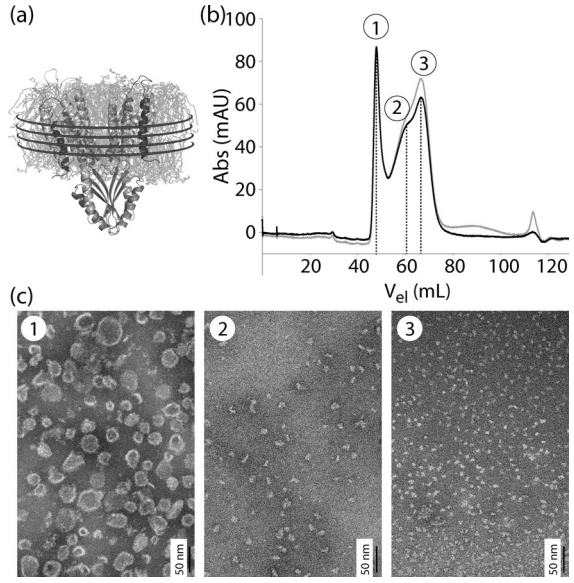

Figure 1. a) CzcD in a nanodisc, based on a homology model using YiiP.[18] b) Size-exclusion chromatogram of SMA_2:1-solubilized CzcD after affinity purification. Elution was followed by measuring the absorption at 280 nm (black) and 260 nm (green). The SMA copolymer shows an absorption maximum around 260 nm. Additional SEC chromatograms are shown in Figure S3. c) Negative-stain transmission electron micrographs of eluted fractions from (b), collected at the indicated positions of the chromatogram (V_{el} = 47 mL, 58 mL, 68 mL). EM images of a sample after magic-angle spinning are shown in Figure S5.

liposome-like particles and may correspond to incompletely solubilized membrane fragments. Electron micrographs from fraction 2 show a relatively non-homogenous population of significantly smaller particles of approximately 15–20 nm in diameter. Finally, a homogenous population of nanodiscs 10–15 nm in size was obtained from the third fraction. Dynamic light scattering experiments of an independent batch with higher homogeneity confirmed these findings (Figure S4). Using a phosphorous assay, we determined that there are 32–35 lipids per protein dimer, which corresponds to about one layer of lipid around the protein (see details in the Supporting Information). Similar lipid/protein ratios were found in previous reports.[8,12]

To explore the possibility of obtaining atomic-resolution NMR information from these native-nanodisc samples of CzcD, we sedimented nanodisc-containing fractions (i.e., peaks 2 and 3 of the chromatogram shown in Figure 1b, or equivalent peaks from other purifications) into a 1.3 mm solid-state NMR sample rotor through ultracentrifugation (about 3 μL sample volume). We used three different isotope-labeling schemes in this study: 1) uniform ^{13}C,^{15}N labeling, 2) uniform ^{2}H,^{13}C,^{15}N labeling, and 3) deuteration and selective labeling of Ile-δ1 sites with CH_3 groups.

Figure 2 shows one-dimensional ^{13}C- and ^{15}N-detected spectra of CzcD in native nanodiscs, providing a first impression of the sample and its composition. The direct-excitation ^{13}C spectrum reveals a number of sharp signals in the aliphatic region (10–60 ppm), as well as in the region of 120–130 ppm, in which olefinic and aromatic carbons resonate, which likely stem from lipids. Furthermore, resonances in the carbonyl (170–180 ppm), aliphatic (10–60 ppm), and aromatic (120–140 ppm) regions can be ascribed to protein signals. In ^{13}C spectra obtained with ^{1}H-^{13}C cross-polarization (CP, Figure 2c), the lipid signals also dominate. The ^{13}C CP spectrum obtained with the deuterated sample (Figure 2d) shows strongly reduced signal intensity compared to the direct-excitation ^{13}C spectrum (Figure 2b) and the CP spectrum of the protonated sample (Figure 2a). This is expected in such ^{1}H-^{13}C CP spectra, owing to the absence of protons; the observed signals, primarily from carbonyl and C^{α} sites, result from cross-polarization from the re-protonated amide H^{N} sites. Finally, the ^{15}N spectrum (Figure 2e,f) reveals an intense backbone amide signal, as well as signals corresponding to His, Arg, and Lys side chains. We also collected INEPT-based correlation experiments, which detect only highly flexible C–H sites. This spectrum shows only lipid signal, thus suggesting that CzcD is devoid of extended stretches of highly flexible residues (see Figure S6 in the Supporting Information).

We next investigated the dynamic properties of CzcD in native nanodiscs. At this stage we were interested in overall properties, and in particular the question of whether nanodisc-embedded CzcD undergoes fast axial rotation inside the nanodisc (which itself is immobilized because of the sedimentation brought about by MAS). Such axial rotation has been shown for several membrane proteins in liposomes.[20,21] The presence of fast axial rotation is expected to strongly reduce dipolar order parameters. Strictly speaking, the dipolar coupling of ^{1}H-^{15}N bonds that are parallel to the rotation axis is not reduced, but often an overall reduction by approximately a factor 2 is seen, even for proteins with no extramembrane domains (see Refs. [21,22]). In CzcD, which has a cytoplasmic domain, the N–H bonds are distributed almost uniformly, such that overall rotation would result in significant reduction of the dipolar coupling. If such overall rotation of the molecules occurs on a nanosecond-to-microsecond timescale, the ^{15}N $R_{1\rho}$ spin relaxation rate constants are expected to be enhanced. Finally, R_1 relaxation rate constants are sensitive to motions if they occur on shorter (ps to ns) timescales. We thus performed bulk measurements of these three dynamic parameters, integrated over all amide signals, using robust approaches based on deuterated protein and high MAS frequency (Figure 2h,g and Figure S7). The dynamics measurements reveal that CzcD does not undergo fast axial rotation in nanodiscs: the H-N dipolar order parameters are fairly high ($S \approx 0.8$, Figure 2h), which presumably reflects mostly local motion in an otherwise rigid molecular frame. These order parameters are slightly lower than those found in crystalline proteins that undergo only local motions (where $S \approx 0.85$–0.9). Interestingly, this finding also suggests that the cytoplasmic domain does not undergo large-scale motion with respect to the transmembrane domain. Likewise, both R_1 and $R_{1\rho}$ rate constants are similar to values found in microcrystalline proteins[23] that are devoid of overall motion. These parameters do not show significant temperature dependence over the probed temperature range (270–298 K, Figure 2i). The apparent absence of overall rotation appears reasonable considering the large size of the CzcD dimer and the relatively low lipid/protein ratio (see

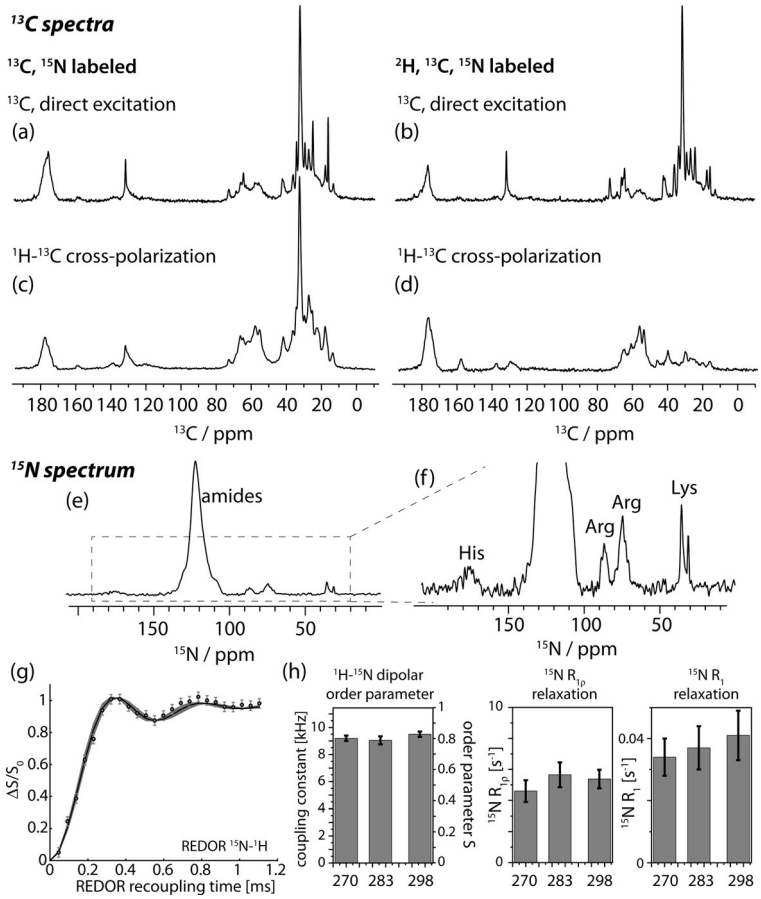

Figure 2. 1D NMR characterization of nanodisc-embedded CzcD. ^{13}C and ^{15}N solid-state NMR spectra of [^{13}C,^{15}N]- (a,c,e,f) and [^{2}H,^{13}C,^{15}N]-labeled (b,d) CzcD in native nanodiscs, recorded at 55 kHz MAS frequency at 14.1 T static magnetic field strength (600 MHz ^{1}H Larmor frequency). g) REDOR measurement of the bulk ^{1}H-^{15}N dipolar order parameter. A single-fit parameter, the effective coupling constant, is invoked in this fit. h) Fitted parameters of dipolar couplings, the order parameters derived from the dipolar couplings, and ^{15}N relaxation rate constants. Further details are provided in Figure S8.

above). The apparent absence of large-scale ns–µs motions (low $R_{1\rho}$ rate constants) leads us to predict that the transverse relaxation time constants (T_2') are also long. Since line widths depend on these coherence lifetimes, this is an important parameter. Indeed, we find relatively long T_2' lifetimes on the order of 25–30 ms for ^{15}N and $^{13}C'$, and about 4 ms for ^{1}H (see Table S2). Although crystalline proteins typically show slower coherence decays (by a factor of around 2–3; see Ref. [24] and Table S2), our data suggest that it should be possible to obtain high-resolution spectra for nanodisc-embedded CzcD.

To evaluate the potential of obtaining such atomic-resolution information, we then performed three-dimensional ^{1}H-^{15}N-^{13}C correlation experiments. With a molecular weight of 2×34 kDa, the CzcD dimer is a very large protein for ssNMR applications, and the corresponding spectral complexity and sensitivity penalty make 3D ssNMR spectroscopy challenging. To our knowledge, no protein of this size, including non-membrane proteins, has been assigned by ssNMR to date, thus highlighting this challenge. As an additional complication, the sample amount is often limited, particularly for membrane proteins. For the case of CzcD, we obtained about 1–4 mg of protein per liter of culture; traditional ssNMR approaches with ^{13}C-detection typically require 10–20 mg of protein. With these requirements in terms of sensitivity and resolution in mind, we turned to deuteration and selective re-protonation of amide or methyl sites, combined with fast-MAS and proton-detected experiments, for high detection sensitivity and resolution. Indeed, we were able to obtain three-dimensional H-N-C spectra at fast (55 kHz) MAS within 3.5–5 days (see the Methods section in the Supporting Information). Figure 3a shows a hCANH experiment that correlates the amide proton and nitrogen frequencies to the intraresidue C^{α}, and Figure 3b shows a hCONH experiment,[25] which connects the amide moiety to the C′ of the preceding residue. Projections of these 3D spectra, and further 2D planes thereof, are shown in Figure S9. Typical amide ^{1}H line widths are of the order of 50–70 Hz, which is narrower than line widths obtained with 2D crystals of β-barrel membrane proteins,[26] or a sample of liposome-embedded proteorhodopsin (a protein that yields highly resolved ^{13}C-detected spectra).[27] ^{1}H line widths of methyl groups obtained through CH_3 labelling[28] of Ile-δ1 sites are as low as around 30–40 Hz (Figure 3c). Notwithstanding these fairly favorable line widths, the large number of residues (more than 300) leads to severe resonance overlap, which hampers assignment and makes it difficult to evaluate the completeness of these spectra.

In order to assist the assignment, we prepared samples of the isolated cytoplasmic (soluble) C-terminal domain ($CzcD_{209\text{-}316}$) and obtained solution-state NMR assignments with and without zinc (see Figure S7). Solution-state diffusion-ordered spectroscopy showed that in the presence of two equivalents of zinc, the protein dimerizes. With these assignments in hand, we identified 13 spin systems, in 3 stretches of the cytoplasmic domain, which closely match in the four frequencies we observe (^{1}H, ^{15}N, $^{13}C^{\alpha}$ and $^{13}C'$) to resonance peaks in the full-length ssNMR spectrum (6 of which are shown in Figure 3a,b), thereby allowing the transfer of assignments. Interestingly, the closest similarity is found to the spectra of the Zn^{2+} form (Table S3). This finding suggests that full-length CzcD in nanodiscs is in a Zn^{2+}-bound and presumably dimeric form, as expected from the available crystal structures. We note that for membrane proteins of more than 300 residues, assignment remains challenging in terms of resolution and sensitivity, and further 3D experiments in addition to the two experiments shown here will be required for unambiguous assignment.

Figure 3c compares the methyl HC correlation spectra of soluble and full-length proteins. The relatively large number of expected cross-peaks (20 in the TM part and 4 in the cytoplasmic domain), and the fact that methyl groups in TM parts tend to experience very similar environments and thus

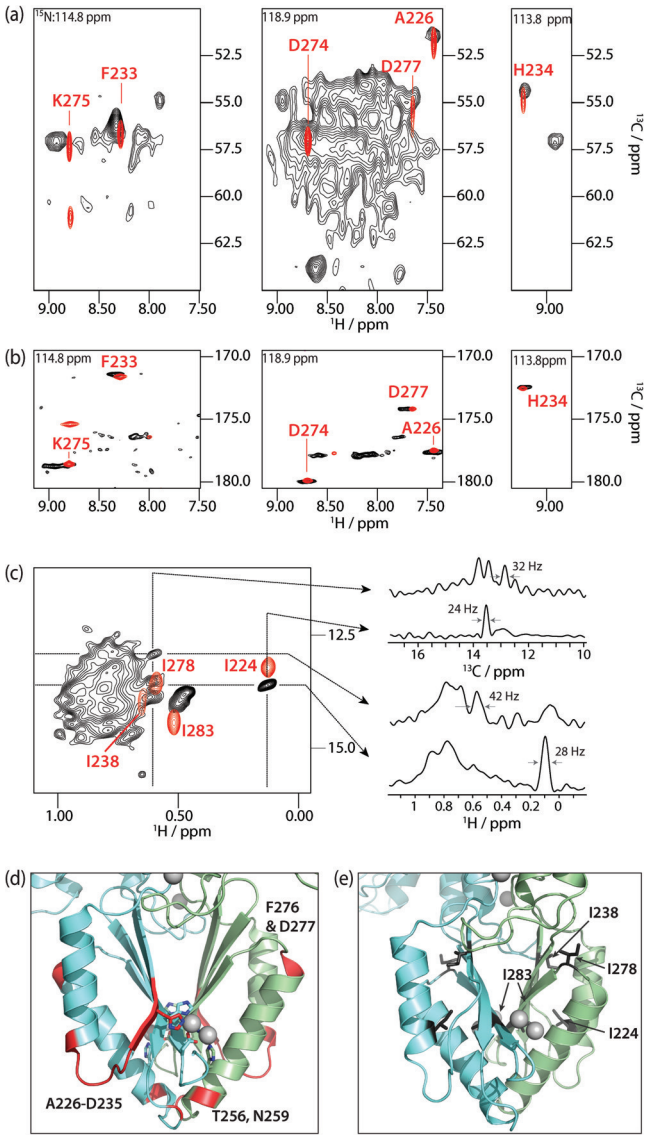

Figure 3. Proton-detected 3D (a,b) and 2D (c) spectra of nanodisc-embedded deuterated CzcD. a) hCANH and b) hCONH correlation spectrum of [^{2}H,^{13}C,^{15}N] CzcD obtained at 600 MHz ^{1}H Larmor frequency and 55 kHz MAS frequency. In addition to the ssNMR spectra (black), solution-state spectra of the soluble domain (red) are overlaid. Further views of these spectra are provided in Figure S9. c) 2D ssNMR HC spectrum of u-[^{2}H^{12}C],Ile-δ1-[^{13}CH$_3$] CzcD (black) and solution-state ^{13}C-HSQC from the [^{13}C,^{15}N] soluble domain (red). In all cases, the soluble-domain spectra were obtained from a sample containing a two-fold molar excess of Zn^{2+}. d) Location of the residues identified in the 3D spectra of panels mapped on the YiiP crystal structure (a, b). e) Localization of the Ile side chains in the cytoplasmic domain within a CzcD homology model.

similar chemical shifts, limits resolution. Nonetheless, the assigned Ile cross-peaks from the soluble domain can be identified in the full-length CzcD, and they appear distinct from the TM Ile peaks (Figure 3c). Interestingly, these methyl resonances show some chemical-shift differences to the isolated cytoplasmic domain, thus suggesting that the presence of the TM domain and the lipid bilayer alters the packing of the dimerizing cytoplasmic domains.

To summarize, we have shown that membrane proteins directly extracted from the bacterial membrane using SMA polymers can be studied by MAS ssNMR spectroscopy, thus opening the way for ssNMR studies of these challenging proteins. The present example of a 2 × 34 kDa cation diffusion facilitator protein shows that favorable line widths are obtained, enabling high-resolution studies. This approach does not require conventional detergents in any step, which is an advantage over nanodiscs based on membrane-scaffold proteins, which have also been used for NMR studies.[29,30] The low amount of co-purified lipid may reflect a more limited environment than the native membrane, however this also leads to an enrichment of the protein mass fraction in the ssNMR rotor, thereby leading to increased sensitivity. The lipids that are extracted with the protein have the same isotope labeling as the protein, thus giving deuterated lipids for enhanced sensitivity and resolution without any excess cost.[26] Native nanodiscs may also be an interesting alternative to recently reported NMR approaches performed with native membrane preparations or whole cells.[31,32] These "in-membrane NMR" approaches allow the study of over-expressed proteins directly in the membrane, but they suffer from the low amounts of target protein and from the presence of other membrane proteins. Native nanodiscs overcome these limitations, since the target protein can be affinity-purified and thus enriched in a form that is stable on the time scales of NMR experiments. We believe that this approach is versatile: SMA can extract membrane proteins (α-helical, β-barrels) either from the native membrane or reconstituted liposomes.[16] Properties important for NMR sensitivity, such as the lipid/protein ratio, are similar in these other reported cases, thus suggesting that the favorable ssNMR properties revealed in this study are likely general and would also apply to other SMA-nanodisc-embedded proteins.

Acknowledgements

We thank Prof. Sandro Keller, Jessica Klement, Dr. Vilius Kurauskas, and Katharina Weinhäupl for insightful discussions. We thank Daphna Fenel and Dr. Christine Moriscot for the collection of electron-microscopy data. This work was supported by the European Research Council (ERC-StG 311318-ProtDyn2Function), the CEA, CNRS and Université Grenoble Alpes. J.M.D. and J.A.K. acknowledge financial support via the Seventh Framework Program of the European Union (Marie Curie Initial Training Network "ManiFold", Grant No. 317371). We thank Polyscope for their kind gift of SMA. This work used the platforms of the Grenoble Instruct Center (ISBG; UMS 3518 CNRS-CEA-UJF-EMBL) with support from FRISBI (ANR-10-INSB-05-02) and GRAL (ANR-10-LABX-49-01) within the Grenoble Partnership for Structural Biology (PSB). The electron microscope facility is supported by the Rhône-Alpes Region, the Fondation Recherche Medicale (FRM), the fonds FEDER, and the GIS-Infrastructures en Biologie Sante et Agronomie (IBISA).

Conflict of interest

The authors declare no conflict of interest.

Keywords: coplymers · membrane proteins · nanodiscs · NMR spectroscopy · solid-state NMR

How to cite: *Angew. Chem. Int. Ed.* **2017**, *56*, 2508–2512
Angew. Chem. **2017**, *129*, 2549–2553

[1] M. Zoonens, J. Comer, S. Masscheleyn, E. Pebay-Peyroula, C. Chipot, B. Miroux, F. Dehez, *J. Am. Chem. Soc.* **2013**, *135*, 15174–15182.
[2] H.-X. Zhou, T. A. Cross, *Annu. Rev. Biophys.* **2013**, *42*, 361–392.
[3] J. L. Popot, T. Althoff, D. Bagnard, J. L. Banères, P. Bazzacco, E. Billon-Denis, L. J. Catoire, P. Champeil, D. Charvolin, M. J. Cocco, et al., *Annu. Rev. Biophys.* **2011**, *40*, 379–408.
[4] U. H. N. Dürr, M. Gildenberg, A. Ramamoorthy, *Chem. Rev.* **2012**, *112*, 6054–6074.
[5] A. Nath, W. M. Atkins, S. G. Sligar, *Biochemistry* **2007**, *46*, 2059–2069.
[6] M. C. Orwick, P. J. Judge, J. Procek, L. Lindholm, A. Graziadei, A. Engel, G. Gröbner, A. Watts, *Angew. Chem. Int. Ed.* **2012**, *51*, 4653–4657; *Angew. Chem.* **2012**, *124*, 4731–4735.
[7] A. R. Long, C. C. O'Brien, K. Malhotra, C. T. Schwall, A. D. Albert, A. Watts, N. N. Alder, *BMC Biotechnol.* **2013**, *13*, 41.
[8] T. J. Knowles, R. Finka, C. Smith, Y.-P. Lin, T. Dafforn, M. Overduin, *J. Am. Chem. Soc.* **2009**, *131*, 7484–7485.
[9] I. D. Sahu, R. M. McCarrick, K. R. Troxel, R. Zhang, H. J. Smith, M. M. Dunagan, M. S. Swartz, P. V. Rajan, B. M. Kroncke, C. R. Sanders, et al., *Biochemistry* **2013**, *52*, 6627–6632.
[10] S. Gulati, M. Jamshad, T. J. Knowles, K. A. Morrison, R. Downing, N. Cant, R. Collins, J. B. Koenderink, R. C. Ford, M. Overduin, et al., *Biochem. J.* **2014**, *461*, 269–278.
[11] S. Paulin, M. Jamshad, T. R. Dafforn, J. Garcia-Lara, S. J. Foster, N. F. Galley, D. I. Roper, H. Rosado, P. W. Taylor, *Nanotechnology* **2014**, *25*, 285101.
[12] V. Postis, S. Rawson, J. K. Mitchell, S. C. Lee, R. A. Parslow, T. R. Dafforn, S. A. Baldwin, S. P. Muench, *Biochim. Biophys. Acta Biomembr.* **2015**, *1848*, 496–501.
[13] M. Jamshad, J. Charlton, Y.-P. Lin, S. J. Routledge, Z. Bawa, T. J. Knowles, M. Overduin, N. Dekker, T. R. Dafforn, R. M. Bill, et al., *Biosci. Rep.* **2015**, *35*, 1–10.
[14] J. M. Dörr, M. C. Koorengevel, M. Schäfer, A. V. Prokofyev, S. Scheidelaar, E. A. W. van der Cruijsen, T. R. Dafforn, M. Baldus, J. A. Killian, *Proc. Natl. Acad. Sci. USA* **2014**, *111*, 18607–18612.
[15] D. J. K. Swainsbury, S. Scheidelaar, R. van Grondelle, J. A. Killian, M. R. Jones, *Angew. Chem. Int. Ed.* **2014**, *53*, 11803–11807; *Angew. Chem.* **2014**, *126*, 11997–12001.
[16] J. M. Dörr, S. Scheidelaar, M. C. Koorengevel, J. J. Dominguez, M. Schäfer, C. A. van Walree, J. A. Killian, *Eur. Biophys. J.* **2016**, *45*, 3–21.
[17] A. Anton, C. Grosse, J. Reissmann, T. Pribyl, D. H. Nies, *J. Bacteriol.* **1999**, *181*, 6876–6881.
[18] M. Lu, J. Chai, D. Fu, *Nat. Struct. Mol. Biol.* **2009**, *16*, 1063–1067.
[19] N. Coudray, S. Valvo, M. Hu, R. Lasala, C. Kim, M. Vink, M. Zhou, D. Provasi, M. Filizola, J. Tao, et al., *Proc. Natl. Acad. Sci. USA* **2013**, *110*, 2140–2145.
[20] B. B. Das, H. J. Nothnagel, G. J. Lu, W. S. Son, Y. Tian, F. M. Marassi, S. J. Opella, *J. Am. Chem. Soc.* **2012**, *134*, 2047–2056.
[21] W. Luo, S. D. Cady, M. Hong, *Biochemistry* **2009**, *48*, 6361–6368.
[22] S. H. Park, B. B. Das, F. Casagrande, Y. Tian, H. J. Nothnagel, M. Chu, H. Kiefer, K. Maier, A. A. De Angelis, F. M. Marassi, et al., *Nature* **2012**, *491*, 779–783.
[23] J. D. Haller, P. Schanda, *J. Biomol. NMR* **2013**, *57*, 263–280.
[24] L. B. Andreas, T. Le Marchand, K. Jaudzems, G. Pintacuda, *J. Magn. Reson.* **2015**, *253*, 36–49.
[25] E. Barbet-Massin, A. J. Pell, J. S. Retel, L. B. Andreas, K. Jaudzems, W. T. Franks, A. J. Nieuwkoop, M. Hiller, V. Higman, P. Guerry, et al., *J. Am. Chem. Soc.* **2014**, *136*, 12489–12497.
[26] R. Linser, et al., *Angew. Chem. Int. Ed.* **2011**, *50*, 4508–4512; *Angew. Chem.* **2011**, *123*, 4601–4605.
[27] M. E. Ward, L. Shi, E. Lake, S. Krishnamurthy, H. Hutchins, L. S. Brown, V. Ladizhansky, *J. Am. Chem. Soc.* **2011**, *133*, 17434–17443.
[28] V. Kurauskas, E. Crublet, P. Macek, R. Kerfah, D. F. Gauto, J. Boisbouvier, P. Schanda, *Chem. Commun.* **2016**, *52*, 9558–9561.
[29] F. Hagn, M. Etzkorn, T. Raschle, G. Wagner, *J. Am. Chem. Soc.* **2013**, *135*, 1919–1925.
[30] A. Z. Kijac, Y. Li, S. G. Sligar, C. M. Rienstra, *Biochemistry* **2007**, *46*, 13696–13703.
[31] M. Renault, R. Tommassen-van Boxtel, M. P. Bos, J. A. Post, J. Tommassen, M. Baldus, *Proc. Natl. Acad. Sci. USA* **2012**, *109*, 4863–4868.
[32] T. Jacso, W. T. Franks, H. Rose, U. Fink, J. Broecker, S. Keller, H. Oschkinat, B. Reif, *Angew. Chem. Int. Ed.* **2012**, *51*, 432–435; *Angew. Chem.* **2012**, *124*, 447–450.

Manuscript received: October 25, 2016
Revised: December 13, 2016
Final Article published: January 27, 2017

